Mar Biol (2010) 157:505–514
DOI 10.1007/s00227-009-1336-5

ORIGINAL PAPER

Orientation affects the sensitivity of *Acartia tonsa* to fluid mechanical signals

David M. Fields

Received: 10 April 2009 / Accepted: 28 October 2009 / Published online: 17 November 2009

Abstract Nearly all organisms show directional bias in sensitivity to environmental signals. In this study, the behavioral sensitivity of a common estuarine copepod, *Acartia tonsa*, varies significantly with respect to their orientation to a well-characterized fluid mechanical signal. Maximum sensitivity occurs at an angle of 25°–30° and lowest sensitivity occurs at angles of 60°–90° relative to the source. These results support the hypothesis that copepods are not uniformly sensitive to fluid signals and show directional bias in mechanosensitivity. The data also show that large copepods initiate their escape reaction further from the source than small copepods. There is, however, an uncharacteristically large increase in sensitivity at the transition between the nauplii and C1 stage despite being similar in size. This suggests that the mechanosensory system of the naupliar stages is less sensitive to fluid signals and helps to explain the higher predation rates experienced by nauplii.

Introduction

The spatial orientation of the prey is an important, but often ignored, component of predator–prey interactions. In evaluating the outcome of predator–prey interactions, most studies examine the susceptibility to predation based on their location within the predator's perceptive field (e.g. the angle of a prey from the sensor of the predator). The data are then used to map the sensory field of the predator for a specific prey type (Fields and Yen 1996; Doall et al. 2002). However, within a given location relative to the predator, the prey's orientation can vary considerably depending on its distribution of mass (Fields and Yen 1997b; Jiang and Strickler 2005), feeding current structure (Fields and Yen 1993; Bundy and Paffenhofer 1996) and ambient fluid motion (Fields and Yen 1997b). To date, relatively little attention has been given to understanding the potential effects of the spatial orientation of the prey on their ability to detect and avoid predators. Yet prey susceptibility is a product of both the ability of the predator to detect and attack a prey and the prey's ability to detect and avoid an attack.

If a potential prey item can detect an attacking predator with equal sensitivity from all directions, than their orientation within a particular position in predators sensory field will be of little consequence to their escape success. However, if prey have greater sensitivity in one orientation over another, then the attack angle relative to the preys' orientation (and not only distance and position relative to the predator) will have important consequences for its ability to detect and escape predation. Limited directional sensitivity can leave the prey with sensory "blind" spots making them more susceptible to predatory attacks that are initiated from a particular direction. For example, predators that attack prey that use vision are more successful when they approach from a direction where the prey has limited vision (e.g. from behind). Similarly, chemoreceptive prey are more likely to be captured by a predator approaching from downwind (downstream) rather than upwind (upstream). For rheotactic organisms, the existence or location of "blind" spots remains unexplored. However, there is circumstantial evidence from morphological and physiological data to suggest that both terrestrial and aquatic organisms may have mechanoreceptive "blind" spots in their sensory field. For example, insects such as

Communicated by M. A. Peck.

D. M. Fields (✉)
Bigelow Laboratory for Ocean Sciences,
West Boothbay Harbor, ME 04575, USA
e-mail: dfields@Bigelow.org

cockroaches (Dagan and Parnas 1970) and crickets (Insausti et al. 2008) possess air motion sensitive mechanoreceptors at the end of their abdomen and at the head of the animal. When stimulated by the air motion caused by a fast approaching predator, from either the rear or head, the prey initiates an escape reaction. Attacks from the side, however, appear less informed to the prey. Recent literature suggests that predators of crickets (Eutruscan shrew) may exploit a sensory weakness by attacking almost exclusively from the side (Anjum et al. 2006). Similar sensory biases are also prevalent in crayfish, which may be driving higher attack rates from side (Herberholz et al. 2004).

Copepods detect other organisms, including predators, primarily through mechanoreception (Fields and Yen 2002). Although there are no studies that examine the sensitivity of the posterior region of copepods, it is likely that the long setae on the caudal region are innervated similar to lobsters and crayfish, providing sensory information of an approaching predator. Positioned at the front of the animal are two highly innervated antennae. Copepod antennae are a linear array of approximately 100 mechanoreceptive setae (Huys and Boxshall 1991; Kurbjeweit and Buchholz 1991; Yen et al. 1992). Because they are organized in a linear fashion, their sensitivity to fluid motion is inherently biased by its orientation in the flow. Such a structure is analogous to the oceanographic deployment of a series of flow meters connected linearly along a single tether. If the array is deployed vertically in the water column, it will detect velocity gradients with depth in the water column. If the array is deployed horizontally in the water column with all sensors at a single depth, it will best detect velocity gradients in the horizontal direction. This suggests the relative orientation of the copepod's antennae within a larger hydrodynamic feature should impact its ability to detect flow from particular directions.

In this study, experiments were conducted to directly test if orientation affects the escape distance of laboratory raised *Acartia tonsa* from a temporally stable and well-described fluid disturbance.

Methods

Animal collection

Brood stock of *Acartia tonsa* was collected and sorted from the pier at Bigelow Laboratory for Ocean Sciences (BLOS: 43°50′N–69°38′W). Cultures were maintained at 17–18°C on a mixed diet of *Rhodomonas lens, Isochrisis galabana and Thalasiosira pseudonana*. Stock algal cultures were acquired from the Culture Collection of Marine Phytoplankton (CCMP) at Bigelow Laboratory and raised on f/2 media under continuous light at 18°C.

Video recordings

Video observations were made through a 1-l Plexiglas vessel. A cube of approximately 90–100 ml of fluid in the experiment tank (Fig. 1) was filmed for analysis using a magnification of 12–20X. The filming apparatus was arranged as a modified Schlieren optical pathway (Fields and Yen 1993). The video cameras consisted of two perpendicularly mounted Hitachi cameras equipped with 105-mm Nikon lenses. In this way, the X Z coordinates and the Y Z views of both the copepods and the siphon were obtained. Filming simultaneously from two perpendicularly mounted cameras provided three-dimensional coordinates of all object within the field of view. The filming volume was illuminated using two Melles Griot 632-nm helium neon lasers each expanded and collimated to 50 mm using an Oriel (Newport, Stratford, CT, USA)

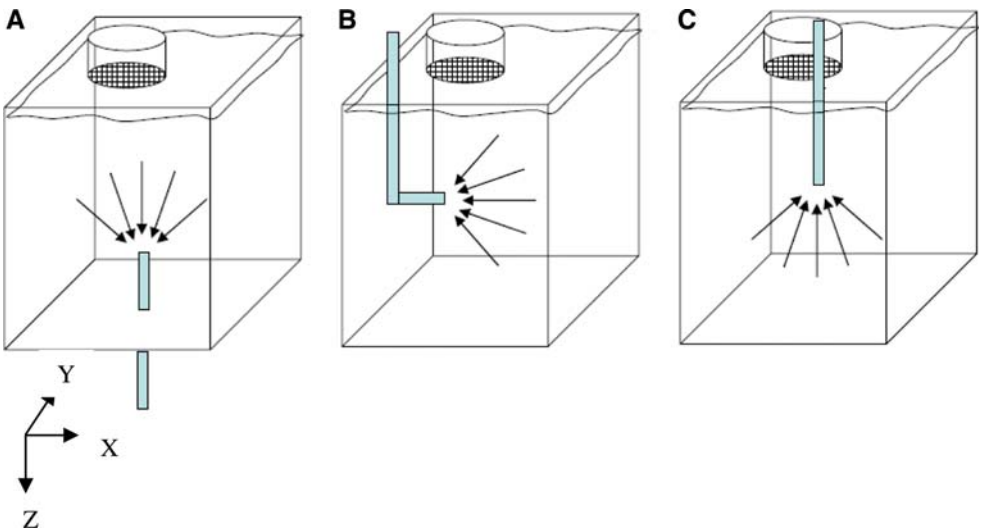

Fig. 1 Siphon configurations used to evoke the escape reaction in *Acartia tonsa*. Siphons (1 mm OD) were oriented **a** vertical upward, **b** horizontal, **c** vertical downward position. Flow rates through the siphon were maintained at 1.83 ml/min for all configurations

beam expander and collimator. Images were recorded on two Leitch DPS-Digital recording systems synchronized with two Horita time code generators (TRG-50; Mission Viejo, CA, USA). To increase temporal resolution, individual video frames (0.033 s) were analyzed field by field (0.0167 s) using NIH-Image Analysis® software.

Siphon tank configuration

A siphon flow was used to create a temporally stable fluid mechanical disturbance. The resulting flow fields are well characterized and have been used previously to analyze copepod escape behavior (Fields and Yen 1996; Kiørboe et al. 1999; Waggett and Buskey 2007). The siphons were constructed from stock Cornix Pyrex glass capillary tubes and mounted in the center of the 1-l tank (Fig. 1). The mouth of the 1-mm (outer diameter) siphon was positioned at a height of ~50 mm from the bottom of the tank. Flow rates for all siphon configurations were 1.83 ml/min. A constant head pressure was maintained by simultaneously replacing the exiting water with 0.45-µm filter seawater. To minimize the disturbance to the siphon flow, incoming water was reintroduced into the tank through a 20-µm mesh screen located just below the water's surface (Fig. 1). The flow rate was chosen such that the majority of escape reactions occurred at a distance of at least 3 mm from the siphon center. This was to ensure that the siphon did not interfere with the determination of the position of the copepod in the video cameras. Since *A. tonsa* are bottom heavy and tend to be oriented vertically within the water column (Fields and Yen 1997b), three different siphon configurations were used: a vertical siphon drawing fluid down, a horizontal siphon and a vertical siphon drawing fluid up (Fig. 1). The observation tank for each siphon configuration was stocked with 200–300 animals. Each escape was treated as an independent measure.

Escape behavior

The appendages (and their motion) involved in an escape reaction have been described for *Cyclops* sp. (Strickler 1975; Lenz and Hartline 1999; Lenz et al. 2004) and *Oithona* sp. (Fields 2000) and can be easily differentiated from a simple flick response or an attack response (Fields and Yen 2002) based on the appendages used. The escape reaction can involve a single jump in which the antennae are drawn to the sides of the body followed by the motion of the swimming legs or a series of jumps in which there is one beat of the first antenna followed by multiple cycles of motion in the swimming legs (Strickler 1975; Fields 2000). Both single and multiple jumps (from a single escape) were used in this analysis. Since the threshold for the escape reaction decrease with multiple sequential escapes (Fields 2000), in cases where the flow re-entrained the same animal after an escape, only the first escape reaction was used for further analysis.

Copepod orientation at the point of escape

Video recordings were analyzed frame by frame to determine at what distance the copepods escaped and their relative orientation to the fluid signal. Although animals escaped from all regions surrounding the siphon, analysis was limited to those animals that escaped within 7° of the midline of the mouth of the siphon (Fig. 2, θ_1). An angle of 7° was chosen as an effort to maximize the number of escape reactions eligible for analysis while limiting the location of the escapes to a relatively small region. By limiting the analysis to only those animals escaping in the "same" location relative to the predator, (the siphon) the independent effect of the prey's orientation (Fig. 2, θ_2) on the escape location could be determined. Based preliminary data, at a distance of 3 mm parallel to the mouth of the siphon, the spatial differences in the fluid velocity were relatively small (<1%) while the number of animals initiating their escape response was sufficiently high. The location and orientation of the copepods were calculated from coordinates taken from the video field just prior to each escape reaction. Four coordinates from each animal were collected using data gathered from both cameras: head (X_1,Y_1,Z_1), caudal furca (X_2,Y_2,Z_2), left (X_3,Y_3,Z_3) and right (X_4,Y_4,Z_4) antennules tips (Fig. 2). The animal's midpoint (MP) was calculated as:

$$\mathrm{MP} = \left(\frac{X_1 + X_2}{2}\right), \left(\frac{Y_1 + Y_2}{2}\right), \left(\frac{Z_1 + Z_2}{2}\right). \quad (1)$$

The coordinates for each video frame was referenced to the siphon by assigning the origin to the midpoint of the siphon. The siphon center was denoted (X_o,Y_o,Z_o) and distance (D) of the escape from the siphon was measured from the midpoint of the siphon mouth to the midpoint of the animal as:

$$D = \sqrt{(X_{\mathrm{mp}} - X_0)^2 + (Y_{\mathrm{mp}} - Y_0)^2 + (Z_{\mathrm{mp}} - Z_0)^2} \quad (2)$$

where (X_{mp}, Y_{mp}, Z_{mp}) represents the three-dimensional location of the copepod's midpoint.

The angle (in degrees) of the midpoint relative to the siphon center (θ_1) was calculated as:

$$\theta_1 = \frac{180}{\pi}\mathrm{ATAN}\left(\frac{((X_1 - X_2)^2 + (Y_1 - Y_2^2))^{\frac{1}{2}}}{(Z_1 - Z_2)^2}\right). \quad (3)$$

The orientation of the animal's antennules relative to midline of the siphon was calculated as:

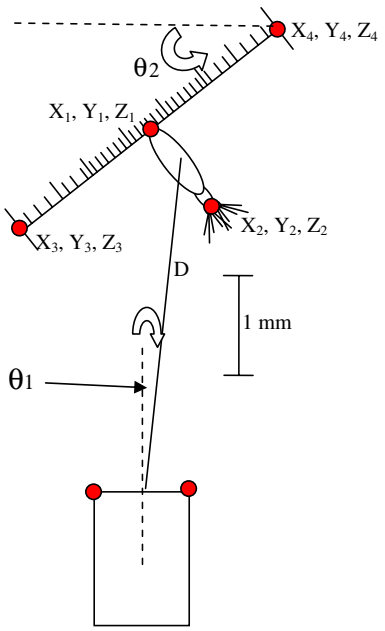

Fig. 2 Data points and coordinate system used to describe the orientation of *Acartia tonsa*. *Dots* indicate the six data points taken from the video frame just prior to the initiation of the escape reaction. *Vertical dashed line*s indicate the location of the copepod relative to the mouth of the siphon. Only copepods that were located directly above the siphon ($\theta_1 = 0 \pm 7$) were used in the analysis. The orientation of the copepod (θ_2) and the distance from the siphon was determined for each escape reaction

$$\theta_2 = \frac{180}{\pi}\mathrm{ATAN}\left(\frac{((X_3 - X_4)^2 + (Y_3 - Y_4^2))^{\frac{1}{2}}}{(Z_3 - Z_4)^2}\right). \quad (4)$$

The distance (D) of the escape reaction from the siphon was plotted as a function of the copepod's orientation θ_2 (Fig. 2) with three possible outcomes: (1) there is no relationship between the orientation of the animals and their escape distance from the siphon. (2) The escape distance is directly proportional to the escape distance (related linearly). (3) The escape distance shows a mid-angle maximum. The effect of orientation on escape distance was evaluated by fitting the data to both a linear regression and a three parameter Gaussian curve (Eq. 5) to test for a mid-angle maximum. Only data that showed a significant slope to either the linear equation or a significant fit to a Gaussian curve allowed rejection of the null hypotheses that orientation of the prey has no effect on the escape distance from the siphon.

$$d = a\mathrm{e}^{-0.5\left[\left(\frac{\theta-\theta_0}{b}\right)^2\right]}. \quad (5)$$

Results

Greater than 99% of the animals initiated an escape response when entrained by the siphon. The few animals that did not escape (6 of 921) were either dead (5 animals) or severely damaged (1 animal). Of the remaining 915 escape reactions, only animals that initiated their escape reaction when located directly in front of the mouth of the siphon ($\theta_1 < \pm 7.0°$) were used for analysis. The body size, antennal orientation (relative to the siphon midline) and the escape location of 17 nauplii (N2-N6) and 82 copepodite through adult (C1-Adult) stages were used in this analysis.

The expected result from the different siphon configurations was to produce a full ±180° range in animal orientation relative to the siphon. However, for the copepods that escaped directly in front of the mouth of the siphon, the orientation angle was never higher than 68° and rarely above 55°. As animals were entrained by the siphon, they were rotated by the spatial gradient in fluid velocity such that their cephalic region pointed away from mouth of the siphon prior to the escape (Fields and Yen 1997b). Even animals drawn from the siphon mounted above the animal rarely initiated their escape reaction until they were oriented with their cephalic region facing away from the siphon center. As a result, only orientations from 0° to ~68° were available for analysis.

Effect of body size on detection distance

Both the nauplii (N2-N6) and copepodite—adult stages of *Acartia tonsa* showed a significant linear relationship between the size of the animal and the distance from the siphon at which they initiated their escape (Table 1; Fig. 3), although both age groups showed considerable variation in their absolute distance from the siphon ($r^2 = 0.24$; $r^2 = 0.19$, respectively). The transition from the nauplii stage to the copepodid stage includes a distinct change in the relative size and orientation of the antennules. Naupliar stage copepods project their small antennules forward and nearly parallel to the body. The copepodids, in contrast, have longer antennules that project nearly perpendicular to the body axis. At this metamorphic transition, copepodids showed greater sensitivity to the siphon flow compared to the similarly sized nauplii. The escape response of the C1 stage was initiated approximately two BL (body lengths) further from the siphon than the nauplii.

The effect of orientation on escape location

Some of the variability in the escape distance for a particular size range of copepod is explained by the orientation of the animal. Copepods were divided into four age groups (N2-N6: C1-C2; C3-C4; C5-adults) and analyzed for the effects of orientation on their escape distance from the tip of the siphon. The orientation of the animal was plotted as a function of the escape distance and fit to both a linear equation and to a simple Gaussian curve (to test for a mid-

Table 1 Statistical results for the linear regression of escape distance as a function of orientation

Stage	Y_o	m	P	N (df)	Adj r^2	Significance
N2-N6						
Linear fit	1,755.5 (125.0)	1.5 (0.6)	0.02	17 (16)	0.25	*
C1-Adult						
Linear fit	1,968.1 (324.7)	2.2 (0.5)	0.001	82 (81)	0.19	***

Y_o is the escape distance intercept, m is the slope, P is the probability, N the number of observations, df is the degrees of freedom, Adj is the mean adjusted correlation

* < 0.05, *** < 0.001

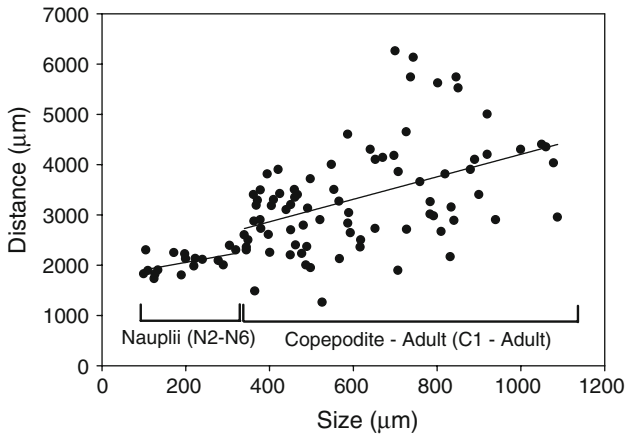

Fig. 3 Escape of *Acartia tonsa* from the suction flow. The data were divided into two groups, naupliar stages and copepodite–adult stages, each independently fit to a linear equation. Despite high variability, linear equations for both data sets are significant. See Table 1

angle maximum). The data for the younger stages (N2-N6 and C1-C2; Table 2) showed no significant effect of orientation on the escape distance. However, in the older stages of *A. tonsa* (C3&C4–C5& adults; Fig. 4) there was a statistically significant effect of orientation on the escape distance. The escape reaction for both age groups occurred at a maximum distance when the copepods were oriented 25°–30° from the siphon. At this angle, the escape reactions for both groups were initiated at over twice the distance of that found at either 0° or 60°.

To determine the interactive effects of animal size (C3-Adult) and orientation, the distance of the escape from the siphon (d) was fit by numerical iteration (Sigma Plot 10; Jandel Software) to a simple 3D Gaussian equation:

$$d = ae^{-0.5\left[\left(\frac{x-x_0}{b}\right)^2+\left(\frac{y-y_0}{c}\right)^2\right]} \quad (6)$$

where a (4,479.0 ± 209.3), b (593.0 ± 133.2), c (35.7 ± 4.7) are calculated constants, and x (923.6 ± 112.2) and y (22.3° ± 2.7°) are the size (µm) and orientation (deg), respectively (Fig. 5 Table 2). For C3 through adult stages, the escape distance was significantly related to copepod size and orientation of the copepod (Table 2). The greatest sensitivity occurred when the animals were oriented at an angle of 20°–30° from the siphon. The lowest sensitivity occurred at 60°.

Table 2 Statistical results for linear and gaussian curve fit to the escape distance as a function of orientation

Stage	P	N (df)	Adj r^2	Significance
N2-N6				
Linear fit	0.02	17 (16)	0.25	*
Gaussian fit	0.30	17 (15)	0.04	NS
C1-C2				
Linear fit	0.36	17 (16)	0.00	NS
Gaussian fit	0.65	17 (15)	0.00	NS
C3-C4				
Linear fit	0.91	40 (39)	0.00	NS
Gaussian fit	0.001	40 (38)	0.28	***
C5-Adult				
Linear fit	0.18	25 (24)	0.34	NS
Gaussian fit	0.009	25 (23)	0.29	**
C3-Adult				
3D Gaussian fit	0.001	82 (77)	0.37	***

P is the probability, N the number of observations, df is the degrees of freedom, Adj is the mean adjusted correlation coefficient

* < 0.05, ** < 0.01, *** < 0.001

Discussion

Copepods detect and respond to spatial gradients in fluid velocity with a variety of behaviors ranging from simple antennule flicks, predatory attacks or escape responses (Fields and Yen 2002). In this study, we have tested whether the orientation of the animal with respect to the 3D spatial gradients in fluid velocity affect the behavioral sensitivity for the escape response in *Acartia tonsa*.

Effect of sensor size on escape threshold

Boxshall et al. (1997) suggested that sensory structures responsible for predator detection (namely the distal tips of the antennules) appear early in development (naupliar stages) and are conserved throughout ontogeny. Individual

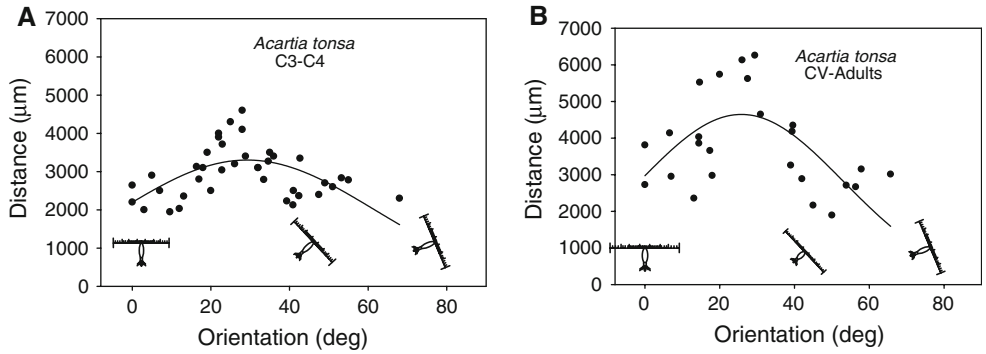

Fig. 4 Escape distance as a function of the orientation (θ_2 in Fig. 2.) of *Acartia tonsa* C3-C4 (**a**) and CV-Adult (**b**). All escape reactions occurred directly in front of the mouth of the siphon ($\theta_1 = 0 \pm 7°$). The data were fit to a 3 parameter Gaussian curve as: $d = ae^{-0.5\left[\left(\frac{\theta-\theta_0}{b}\right)^2\right]}$

antennule segments are added in the proximal region and lengthen as animals develop through the nauplii and copepodid stages to adulthood. This gives rise to an increase in the overall length of the antennule. Assuming all setae have the same sensitivity, the length of the antennule will determine the distance over which a velocity gradient is detected. A small increase in antennule length gives rise to a large difference in the velocities at either end of the antennule, since fluid velocity decays exponentially with distance. Thus, the ability to detect a spatial gradient in fluid velocity should increase with increased antennule span. Yen et al. (1992) reported a fluid velocity threshold of 20 µm s^{-1} for an individual mechanosensor. If we assume that this threshold remains constant, an animal with a 1-mm antennal span (early stage copepodite) can potentially detect a velocity gradient of 20 µm s^{-1}/1 mm (two-dimensional sheared flow of 0.02 s^{-1}). In contrast, an animal with a 2.2-mm antennal span (an adult *Acartia*) theoretically could detect a spatial gradient in velocity of 0.009 s^{-1}. Thus, the different ontogenetic stages would be expected to have a twofold difference in sensitivity to the same velocity gradient, despite having equal sensitivity of the individual mechanosensors.

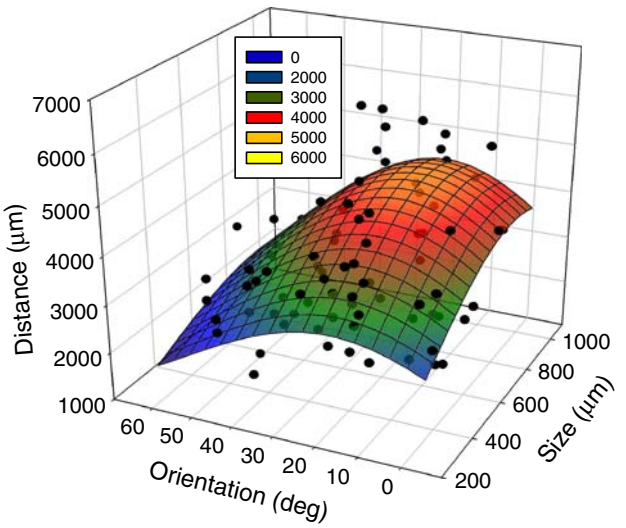

Fig. 5 Escape distance (d) of *Acartia tonsa* C3-adult (600–1,000 µm) from the tip of a siphon as a function of the animal's size (s) and orientation (θ) Data were fit to a 3D Gaussian curve (see text for parameter values, see Table 2 for statistical results)

The data presented in this study shows a significant increase in detection distance with increasing body size. From the C1 to the adult stage, every micron increase in body length gave rise to a 2 micron increase in detection distance. This allowed adults to initiate their escape reaction, on average, 1.6 times further from the siphon than the C1 stage and 2.2 times further than the nauplii stage. The direct relationship between body size and escape distance supports the hypothesis that the higher predation risk of younger stages may be driven in part by their decreased sensitivity to the fluid signals and not just a result of lower escape speeds of the nauplii. These results reinforce previous data for this same species showing that the threshold for an escape reaction of copepod nauplii is much higher than for adult copepods (Fields and Yen 1997a; Kiørboe et al. 1999).

Size, however, did not explain all of the variability in escape distance. Copepods experience a notable morphological change in their antennules, when they metamorphose from the nauliar stage to copepodid stage. Despite the similarity in size, the escape reaction of C1 was initiated at a 27% greater distance than the same-sized N6. There is presently little data on the sensor morphology or physiology of either copepodite or naupliar stage copepods but changes in the antennule architecture is likely to be an important factor determining behavioral sensitivity and warrants further research.

Effect of orientation on escape threshold

Experiments conducted in this study demonstrate that the escape distance varies with the copepod's orientation (θ_2

Fig. 2) within a given hydrodynamic disturbance. These results suggest that *A. tonsa* is not uniformly sensitive to an attack from all directions and have the mechanoreceptive equivalent of "blind spots" to attacks from particular angles. C5 to adult *A. tonsa* initiated an escape reaction up to 2BL further away from the siphon when oriented at an angle of 20°–30° (from vertical) than when oriented at 0° and up to 3 BL further away than when oriented at 60° Directional sensitivity results from a combination of the directional bias of the individual mechanoreceptors (Fields et al. 2002; Fields and Weissburg 2004 and references therein) and their distribution as a linear array of flow sensors along the antennule (Huys and Boxshall 1991; Kurbjeweit and Buchholz 1991; Yen et al. 1992; Fields et al. 2002). What remains unclear, however, is why the relationship between orientation and escape distance shows a mid-angle maximum. If the individual setae showed no directional bias, maximum sensitivity to spatial gradients in flow would be achieved when the antennules were perpendicular to the flow. As the angle of the antennules increased, the projected area exposed to the laminar flow should decrease as a cosine function. The effect should be similar to decreasing the antennal span. However, rather than showing a decline in behavioral sensitivity with angle declination, the escape distance was maximum when animals were oriented between 20° and 40° from vertical. Part of the explanation lies in the directional sensitivity of the individual sensors driven by supporting structures surrounding the sensor or the shape of the sensor itself. For example, a cuticular socket, housing individual setae can restrict the motion of the sensor to a particular direction (Laverack 1976; Weise 1976; Ball and Cowan 1977; Tazaki 1977; Yen et al. 1992). Alternatively, a morphological features such as a bend in the setae provides asymmetrical structural rigidity that limits directional movement (Fields and Weissburg 2005), while feathered setae are more likely to respond to flow that is perpendicular to the side of the setae with the largest cross-sectional area. Directional sensitivity of individual mechanosensors had been reported for insects (Kumagai et al. 1998; Shimozawa et al. 1998), arachnids (Humphrey and Barth 2007) and other copepod species (Fields et al. 2002).

Strong predation pressure has been cited as the evolutionary cause for behavioral (diel vertical migrations (Enright and Hamner 1967), morphological (cyclomorphosis—Brooks 1946) and neurophysiological adaptations (myelinated neurons—Weatherby et al. 2000; rapid firing rates—Fields and Weissburg 2004) in planktonic crustaceans. In this context, it is worthwhile considering the selective pressures that may drive copepods to maintain a particular orientation in the water column. The orientation adopted by an organism is not random. The orientation is due to either the behavioral characteristics and/or the results from the interaction between the morphology of the organism and the frictional forces of the fluid environment (air or water, Jonsson et al. 1991). For example, the stable sinking orientation arises from the balance of two forces: the rotational force due to the separation of the center of mass and the geometric center, and the frictional force between the animal and the surrounding, moving fluid (Vogel 1981; Jonsson et al. 1991). Although there are only a few empirical measurements for most organisms, the geometric center and the center of mass within the body are not identical. This separation creates a lever arm that rotates the organism around the geometric center until it is heavy side down. This provides organism with a stable orientation (Kessler 1985). Passive geotactic mechanisms have been found in bivalve larvae (Jonsson et al. 1991), ciliates (Roberts 1970), algae (Kessler 1985), echinoderm larvae (Pennington and Strathmann 1990) and copepods (Fields and Yen 1997a). Pennington and Strathmann (1990) speculate that echinoderm larvae have evolved such passive mechanisms to aid in feeding. *Acartia tonsa* as are many copepod species (Fields and Yen 1997a; see Jiang and Strickler 2005 for exception) are bottom heavy, maintaining a vertical position in the water column with their antennules positioned parallel to surface. The results of this study suggest that when copepods are vertically oriented in the water column, their most distant escape reactions occur when they are attacked from angles of 20°–30° from the vertical. In contrast, when copepods are attacked from the side (0°), they have the highest susceptibility to being captured (they initiate their escape when the predator is the closest). Thus, all things being equal, an attack would be most profitable to the predator if they approached the copepods from the side (0°). However, the visibility of planktonic prey to a visual predator is strongly affected by the visual angle (θ_1: Fig. 6) of the prey relative to the approaching predator. Optical measurements suggest that in down-welling light, pigmented planktonic organisms are most visible (showing the highest contrast) when they are directly above the predator (0° ± 30°: Thetmeyer and Kils 1995) and nearly invisible when viewed from the side. Janssen (1981) suggests that there maybe a second visibility maxima for transparent prey when they are at an angle slightly larger than Snell's window (48.6°). Ambient light from an angle greater than 48.6° comes from the water below and is reflected off the surface thus appearing dark to the fish. In contrast, transparent zooplankton receives light from above, appearing as a brightly lit copepod on an otherwise dark background.

The greater visibility should theoretically drive the predators to initiate the majority of attacks from angle relative to the prey. Observational data support this hypothesis. Janssen (1981) found that blueback herring

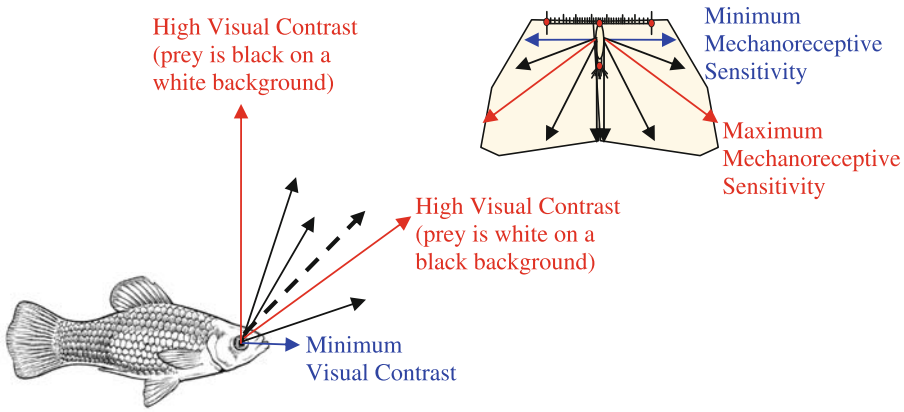

Fig. 6 Cartoon of the perceptive field of a marine copepod (*Acartia tonsa*) and that of a visually based fish predator. The copepod's maximum detection distance for a suction flow occurs at an angle of 20°–30° from the horizontal plane. The maximum detection distance for the visual-based predator (fish) occurs either when its prey is directly above 0° (maximum contrast) or when it is at an angle slightly greater than Snell's window (48.6° from vertical). The average attack angle for planktivorous fish (- - -) occur at ~45°

Alosa aestlvalis attacked planktonic prey along average trajectories of 54° (Fig. 1; θ_1) relative to the fish or 36° (θ_2) relative to the prey. Thetmeyer and Kils (1995) and Batty et al. (1990) report attack angle of 43° and 47° for juvenile and adult herring, respectively, feeding on copepods. Similarly, observations for white crappie (Browman and Obrien 1992a) and golden shiner (Browman and Obrien 1992b) show a predominance of attacks on planktonic prey from angles of ~43°. The results presented in this study suggest that the orientation of copepods in the water column and their greater sensitivity to a mid-angle attack may be an evolutionary response to their higher visibility and hence greater probability of being attacked by visual predators.

Characterizing fluid motion

Determining the specific characteristics of the fluid signal that evokes an escape reaction in copepods is required to understand the ecological implications of different biologically created flow fields. Since copepods are directionally sensitive to a given fluid signal, predicting the behavioral response requires knowledge of both the fluid characteristics and the relative orientation of the animal. When a force is imparted on a fluid volume, the fluid parcel is moved to a new location and is rotated and deformed (Batchelor 1968). For reasons explained in Fields and Yen (1996), the ability to detect movement to the new location requires acute vision and, therefore, is unlikely to be important for the detection of fluid motion by the copepod. Vorticity and deformation, in contrast, provide a potential stimulus for detecting displacement. However, Kiørboe et al. (1999) present convincing evidence that fluid vorticity by itself does not evoke escape reactions. This leads to the conclusion that copepods must respond to fluid deformation. Herein lies the confusion. Fluid deformation describes fluid motion in three-dimensions using single value to describe the magnitude of the deformation. Copepods, in contrast measure fluid motion preferentially within a particular plane. It is this inconsistency between the way fluid signals are characterized, and the way they are detected that has lead to misconceptions about how copepods will respond to given fluid disturbances. The deformation experienced by a small finite volume requires six directional components for complete specification (Batchelor 1968). In Cartesian co-ordinates, the strain rate (S) tensor is given as:

$$S = \begin{pmatrix} \frac{\partial u}{\partial x} & \frac{1}{2}\left(\frac{\partial u}{\partial y} + \frac{\partial v}{\partial x}\right) & \frac{1}{2}\left(\frac{\partial u}{\partial z} + \frac{\partial w}{\partial x}\right) \\ \frac{1}{2}\left(\frac{\partial u}{\partial y} + \frac{\partial v}{\partial x}\right) & \frac{\partial v}{\partial y} & \frac{1}{2}\left(\frac{\partial w}{\partial y} + \frac{\partial v}{\partial z}\right) \\ \frac{1}{2}\left(\frac{\partial u}{\partial z} + \frac{\partial w}{\partial x}\right) & \frac{1}{2}\left(\frac{\partial w}{\partial y} + \frac{\partial v}{\partial z}\right) & \frac{\partial w}{\partial z} \end{pmatrix} \quad (7)$$

where δu, δv, δw are the change in the velocity in the X, Y, Z direction, respectively. In essence, the fluid deformation is the 3D composite of the fluid velocity with respect to space, based on a calculation using all the individual shear tensors shown in the matrix above. The diagonal terms in the matrix (upper left to lower right) are the normal strain terms or the "along streamline strain rate" terms (longitudinal deformation) as referred to by Andrews (1983). The off-diagonal terms represent shear strain rate or the cross-streamline strain rate (pure shear deformation) in each of the three dimensions. Because of viscosity, fluid motion at or below the Kolmogoroff scale (the smallest eddy size) behaves in a correlated manner, motion in one plane simultaneously causes motion in all the other dimensions. Mathematically, the magnitude of the deformation rate is calculated independent of the coordinate system. The direction of the deformation is given by rotating the matrix along the axis that yields the greatest deformation

(commonly referred to as the principle axis of deformation). The coordinate system is oriented such that the maximum strain rate is along one of the axes and the minor strains perpendicular to that axis. Thus, the magnitude of the deformation remains constant regardless of the coordinate system chosen for the analysis. However, at any given instant, the generated flow magnitudes are never equal in all dimensions. Even during isotropic turbulence (where the values are calculated over a long time frame), the instantaneous magnitudes of the strain rate over the 3 dimensions differ. Thus, flow geometries that differ enormously in the orientation of the principle axis of deformation can result in the same magnitude of fluid deformation. Similarly, flows with very different magnitudes of deformation can have equal strain rates in one or several of the component directions. Thus, the deformation rate provides a convenient tool for describing fluid behavior but is not convenient for interpreting the behavior of copepods.

Calculating the threshold deformation for organisms that preferentially detect flow in a particular plane is analogous to calculating the threshold intensity of scattered light for organisms that detect only polarized light within a particular plane. The measured intensity of the signal only provides a maximum value, but the actual threshold for the animal can range from the maximum value to values approaching zero, depending on orientation. Using the deformation, rate is applicable only if one assumes either that the organism detects fluid signals equally in all directions or that they average information over long time scales. For copepods, neither of these assumptions is met and using deformation will inherently leads to high variability in the calculated threshold. Determining the actual threshold requires that the signal be measured in the appropriate plane relevant to the animals individual orientation. These results suggest that previously reported thresholds based on animals in many orientations underestimate the sensitivity of copepods. Furthermore, such generalizations conceal the potential ecological implications of an organism's natural orientation as an antipredatory strategy.

Predator–prey interactions are often the result of generations of interactions. The finality of being eaten provides fertile ground for exploring the subtle interplay involved in the sensory arms race. Such studies require an understanding of the signals, the decay of those signals in space and time and the architecture of the sensory systems involved. More studies aimed at the capabilities of the sensors and how they couple to the physical environment is necessary to appreciate how relatively simple neurological systems can decipher complex and ephemeral signals.

Acknowledgments Thanks to Donald Webster for his constructive criticism. Support for this work was provided by NSF/IOS #0718832 awarded to DM Fields.

References

Andrews JC (1983) Deformation of the active space in the low Reynolds number feeding current of calanoid copepods. Can J Fish Aquat Sci 40:1293–1302

Anjum F, Turni H, Mulder PGH, van de Burg J, Brecht M (2006) Tactile guidance of prey capture in Etruscan shrews. PNAS 103:16544–16549

Ball EE, Cowan N (1977) Ultrastructure of the antennal sensilla of *Acetes* (Crustace, Decapod, Natantia, Sergestidae). Philos Trans R Soc Lond B Biol Sci 277:429–456

Batchelor GK (1968) An introduction to fluid dynamics. Cambridge University Press, Cambridge, p 615

Batty RS, Blaxter JHS, Richard JM (1990) Light intensity and the feeding behaviour of herring, *Clupea harengus*. Mar Biol 107:383–388

Boxshall GA, Yen J, Strickler JR (1997) Functional significance of the sexual dimorphism in the array of setation elements along the antennules of *Euchaeta rimana* Bradford. Bull Mar Sci 61:387–398

Brooks JL (1946) Cyclomorphosis in *Daphnia* I. An analysis of *D. retrocurva* and *D. galeata*. Ecol Monographs 16:409–447

Browman HI, Obrien WJ (1992a) The ontogeny of search behavior in the white crappie *Pomoxis-annularis*. Exp Biol Fish 34(2):181–195

Browman HI, Obrien WJ (1992b) Foraging and prey search behavior of golden Shinner (N*otemigonus-crysoleucas*) larvae. Can J Fish Aquat Sci 49(4):813–819

Bundy MH, Paffenhofer G-A (1996) Analysis of flow fields associated with freely swimming calanoid copepods. Mar Ecol Prog Ser 133:99–113

Dagan D, Parnas I (1970) Giant Fibre and small fibre pathways involved in the evasive response of the American cockroach, *Periplaneta americana*. J Exp Biol 52:313–324

Doall MH, Strickler JR, Fields DM, Yen J (2002) Mapping the attack volume of a free-swimming planktonic copepod, *Euchaeta rimana*. Mar Biol 140:871–879

Enright JT, Hamner WM (1967) Vertical diurnal migration and endogenous rhythmicity. Science 25:937–941

Fields DM (2000) Characteristics of the high frequency escape reactions of *Oithona* sp. Mar Freshw Behav Physiol 34:21–35

Fields DM, Yen J (1993) Outer limits and inner structure: the 3-dimensional flow field of *Pleuromamma xiphias* (Copepoda). Bull Mar Sci 53:84–95

Fields DM, Yen J (1996) The escape behavior of *Pleuromamma xiphias* from a quantifiable fluid mechanical disturbance. In: Lenz PH, Hartline DK, Purcell JE, Macmillan DL (eds) Zooplankton: Sensory ecology and physiology. Gordan and Breach Publ, Amsterdam, pp 323–340

Fields DM, Yen J (1997a) The escape behavior of marine copepods in response to a quantifiable fluid mechanical disturbance. J Plankton Res 19:1289–1304

Fields DM, Yen J (1997b) Implication of copepod feeding currents on the spatial orientation of their prey. J Plankton Res 19: 79–85

Fields DM, Yen J (2002) Fluid mechanosensory stimulation of behavior from a planktonic marine copepod *Euchaeta rimana* Bradford. J Plankton Res 24:747–755

Fields DM, Shaeffer DS, Weissburg MJ (2002) Mechanical and neural responses from the mechanosensory hairs on the antennule of *Gaussia princeps*. Mar Ecol Prog Ser 227:173–186

Fields DM, Weissburg MJ (2004) Rapid depolarization rates from the antennules of copepods. J Comp Phys A 190:877–882

Fields DM, Weissburg MJ (2005) Evolutionary and ecological significance of mechanosensory morphology: copepods as a model system. Mar Ecol Prog Ser 287:269–274

Herberholz J, Sen MN, Edwards DH (2004) Escape behavior and escape circuit activation in juvenile crayfish during prey–predator interactions. J Exp Biol 207:1855–1863

Humphrey JAC, Barth FG (2007) Medium flow-sensing hairs: biomechanics and models. In: Casas J, Simpson SJ (eds) Insect mechanics and control: Adv insect physiol, vol 34, pp 1–80

Huys R, Boxshall GA (1991) Copepod evolution. Ray Society, London

Insausti TC, Lazzari CR, Casas J (2008) The terminal abdominal ganglion of the wood cricket *Nemobius sylvestris*. J Morphol 269:1539–1551

Janssen J (1981) Searching for zooplankton just outside of Snell's window. Limnol Oceanogr 26:1168–1171

Jiang H, Strickler JR (2005) Mass density contrast in relation to the feeding currents in calanoid copepods. J Plankton Res 27:1003–1012

Jonsson PR, Andre C, Lindegarth M (1991) Swimming behavior of marine bivalve larvae in a flume boundry-layer flow: evidence for near-bottom confinement. Mar Ecol Prog Ser 79:67–76

Kessler JO (1985) Hydrodynamic focusing of motile algal cells. Nature 313:220–318

Kiørboe T, Saiz E, Visser AW (1999) Hydrodynamic signal perception in the copepod *Acartia tonsa*. Mar Ecol Prog Ser 179:97–111

Kumagai T, Shimozawa T, Baba Y (1998) The shape of wind receptor hairs of cricket and cockroach. J Comp Physiol A 183:187–192

Kurbjeweit F, Buchholz C (1991) Structure and suspected functions of antennular sensilla and pores of three Arctic copepods, *Calanus glacialis, Metridia longa, Paraeuchaeta norvegica*. Meeresforsch 33:168–182

Laverack MS (1976) External proprioceptors. In: Mill PJ (ed) Structure and function of proprioceptors in invertebrates. Chapman & Hall, London, pp 1–63

Lenz PH, Hartline DK (1999) Reaction times and force production during escape behavior of a calanoid copepod, *Undinula vulgaris*. Mar Biol 133:249–258

Lenz PH, Hower AE, Hartline DK (2004) Force production during pereiopod power strokes in *Calanus finmarchicus*. J Mar Syst 49:133–144

Pennington JT, Strathmann RR (1990) Consequences of the calcite skeletons of planktonic echinoderm larvae for orientation, swimming, and shape. Biol Bull 179:121–133

Roberts AM (1970) Geotaxis in motile micro-organisms. J Exp Biol 53:687–699

Shimozawa T, Kumagai T, Babba Y (1998) Structural scaling and functional design of cercal wind-receptor hairs of cricket. J Comp Physiol A 183:171–186

Strickler JR (1975) Swimming of planktonic *Cyclops* species (Copepoda, Crustacea): pattern, movements and their control. In: Wu TY-T, Brokaw CJ, Brennan C (eds) Swimming and flying in nature. Plenum Press, New York, pp 599–613

Tazaki K (1977) Nervous responses from mechanosensory hairs on the antennal flagellum in the lobster *Homarus gammarus* (L.). Mar Behav Physiol 5:1–18

Thetmeyer H, Kils U (1995) To see and not be seen: the visibility of predator and prey with respect to feeding behaviour. Mar Ecol Prog Ser 126:1–8

Vogel S (1981) Life in moving fluids. Princeton University Press, Princeton

Waggett RJ, Buskey EJ (2007) Copepod escape behavior in non-turbulent and turbulent hydrodynamic regimes. Mar Ecol Prog Ser 334:193–198

Weatherby TM, Davis AD, Hartline DK, Lenz PH (2000) The need for speed. II. Myelin in calanoid copepods. J Comp Physiol 186:347–357

Weise K (1976) Mechanoreception for near-field water displacements in crayfish. J Neurophysiol (Bethesda) 39:816–833

Yen J, Lenz PH, Gassie DV, Hartline DK (1992) Mechanoreception in marine copepods: electrophysiological studies of the first antennae. J Plankton Res 14:495–512